Bimetallic nanoparticles

DOI: 10.1002/smll.200701196

Synthesis of Ag@AgAu Metal Core/Alloy Shell Bimetallic Nanoparticles with Tunable Shell Compositions by a Galvanic Replacement Reaction

Qingbo Zhang, Jianping Xie, Jim Yang Lee, Jixuan Zhang, and Chris Boothroyd*

The fabrication of metallic nanostructures with controllable shapes and sizes is important in delivering the promise of size- and shape-tunable properties of nanomaterials.[1,2] The properties of nanometals can be further modified by incorporating more than one metallic component into a common particle to form, for example, a bimetallic nanoparticle.[3–5] It has been confirmed that co-operative and synergistic interactions between the metallic components could lead to an overall more useful functionality.[6,7] The bimetallic nanoparticles may be fabricated as alloy nanoparticles where the two constituent metals are mixed at the atomic level[7–13] or as core/shell nanoparticles where the two components are separated by distinct phase boundaries.[6,14–17] It is known that bimetallic nanoparticles with the same overall composition but different composition distributions can exhibit different properties.[16,18] The geometric distribution of the metals within a particle between the two extremes of alloy (maximally mixed) and core/shell (minimally mixed) nanoparticles may therefore be used to increase the versatility in property tuning. In an effort to extend the envelope of possibility further, we will demonstrate the synthesis of a new type of core/shell nanostructure where the core is a pure metal and the shell is the alloy of two metals with adjustable compositions, using the Ag–Au system as an example.

The novel Ag@AgAu bimetallic nanoparticles were produced by the replacement reaction between Ag nanoparticles and $HAuCl_4$.[19–24] The replacement reaction between Ag nanoparticles and common Au precursor salts has been used by several groups to produce hollow nanostructures in the past. It has been demonstrated that different synthesis conditions and structures of the starting Ag nanoparticle templates could lead to different end products.[20,25–27] In this study, the conditions under which the reaction would lead to the formation of core/shell nanoparticles with an alloy shell were identified and the mechanism of formation was elucidated by closely following the evolution of the product particles with high-resolution transmission electron microscopy (HRTEM) and UV/Vis spectroscopy.

Figure 1A shows the TEM image of the as-synthesized Ag nanoparticles. The particles were all spherical with diameters of 18.6 ± 2.3 nm. Figure 1B is the HRTEM image of a typical Ag nanoparticle template. The well-resolved lattice fringes throughout the particle, and the hexagonal symmetry of the fast Fourier transformation (FFT) pattern (inset of Figure 1B), indicate that this was a single-crystal nanoparticle. Figure 1C–F are the TEM images of the AgAu-1, AgAu-2, AgAu-3, and AgAu-4 nanoparticles, respectively. While the outer regions of the AgAu-1 nanoparticles were only slightly darker than the core areas, distinct boundaries demarcating the core and shell regions were clearly visible in the AgAu-2, AgAu-3, and AgAu-4 nanoparticles. The difference in contrast between different parts of a particle indicates that electron scattering was heterogeneous; suggesting that the particles were either core/shell structured or had hollow interiors. As will be shown later, energy dispersive X-ray (EDX) and UV/Vis spectroscopic characterizations of the particles indicated that they were core/shell nanoparticles. The core/shell boundary in the nanoparticles of AgAu-1 was less distinct because the core and shell components were not significantly different in composition. The core/shell structure was also confirmed by HRTEM imaging (Figure 1G). The lattice fringes in the HRTEM image of the particles, and the FFT pattern of the HRTEM image, are indications of the single crystallinity of the core/shell nanoparticles. There were no pinholes in the shell, which are usually found in the shell of hollow nanoparticles.[23,28]

The variations in the composition of the bimetallic particles from the center to the outer regions were analyzed by selected-area EDX. The EDX spectrum of a whole particle (Figure S1 of the Supporting Information) shows the co-existence of Au and Ag. However, while Au and Ag were simultaneously detected in the shell suggesting that the shell was a Ag–Au alloy (Table 1), the Au fraction in the shell was significantly higher than that in the core area (Table 1). The difference in composition between the core and shell regions of the particles is an indication that the particles were core/shell structured and not hollow nanoparticles. For nanoparticles with a hollow interior the composition would have to be uniform throughout. There was also a systematic increase in the Au fraction in the shell of the nanoparticles from AgAu-1 to AgAu-4, indicating tunability of the alloy shell composition through changes of the Ag to $HAuCl_4$ ratio in the starting reaction mixture.

Figure 1H shows the UV/Vis spectra of Ag nanoparticles and the core/shell nanoparticles. Only one peak was found for each of the samples and the absorption maxima varied from 409 nm to 529 nm with the increase in the Au content of the shell. The absorption was caused by the surface plasmon resonance (SPR) of the nanoparticles. Since it has been

[*] Q. Zhang, Prof. J. Y. Lee
Department of Chemical and Biomolecular Engineering
National University of Singapore
10 Kent Ridge Crescent, 119260 (Singapore)
E-mail: cheleejy@nus.edu.sg

J. Xie, Prof. J. Y. Lee
Singapore-MIT Alliance, 4 Engineering Drive 3
National University of Singapore, 117576(Singapore)

Dr. J. Zhang
Department of Material Science and Engineering
National University of Singapore
10 Kent Ridge Crescent, 119260 (Singapore)

Dr. C. Boothroyd
Institite of Materials Research and Engineering,
3 Research Link, 117602 (Singapore)

Supporting Information is available on the WWW under http://www.small-journal.com or from the author.

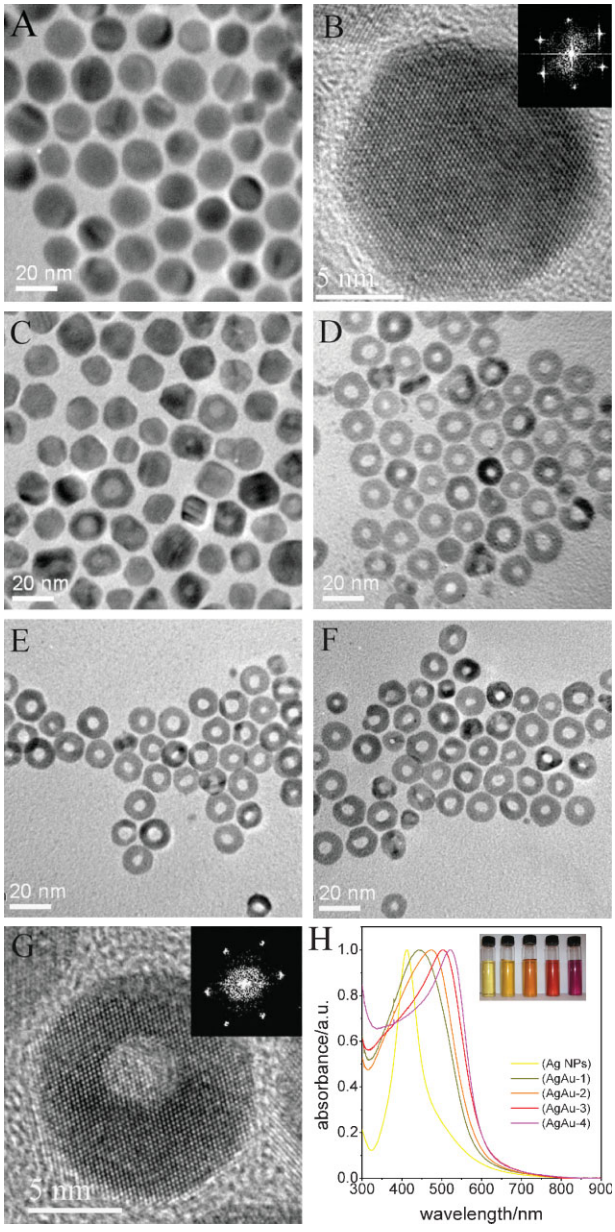

Figure 1. A) TEM image of the Ag nanoparticle seeds; B) HRTEM image of a starting Ag nanoparticle; the inset shows the corresponding diffractogram; C–F)TEM images of AgAu-1 to AgAu-4 nanoparticles; G) HRTEM image of a AgAu-3 nanoparticle; the inset is the corresponding diffractogram; H) normalized absorbance spectra of Ag nanoparticles and AgAu-1 to AgAu-4 nanoparticles; the inset shows the corresponding digital photos.

Table 1. Composition of Ag@AgAu bimetallic nanoparticles.

Nanoparticle	Volume of $HAuCl_4$ solution [mL]	%Au in the shell area	Au% in the core area
AgAu-1	2.80	22.9	10.1
AgAu-2	4.70	51.9	19.2
AgAu-3	5.80	79.4	40.3
AgAu-4	7.00	100	71.2

demonstrated experimentally and by theoretical calculations that the SPR of hollow Au nanoparticles would red shift significantly relative to the SPR of solid Au nanoparticles of the same size,[20,23,29] the observation of absorption maximas at wavelengths *lower* than that of solid Au nanoparticles (≈530 nm) indicates that the particles were not hollow Au nanoparticles. The SPR from the Ag core was totally damped by the relatively thick shell and hence not observable in the spectra.[16] The SPR peaks of the four core/shell samples were all located between the SPR of Ag and Au nanoparticles indicating the presence of a Ag–Au alloy shell.[16]

The conversion of Ag nanoparticles into Ag@AgAu bimetallic nanoparticles involved several sequential processes: oxidative dissolution of Ag atoms, reduction of $AuCl_4^-$ and deposition of Au atoms, counter diffusion of atoms and vacancies, and rearrangement of atoms due to Ostwald ripening.[25,26,28] Although a detailed elucidation of the process may require further work, a phenomenological model may nevertheless be proposed based on the evolution of bimetallic nanoparticles as characterized by HRTEM and UV/Vis spectroscopy. The rates of these processes on different sites of the particles were different and time varying. The sites of action and the principal steps in the overall transformation process are outlined in Scheme 1 to provide a plausible rationalization of the experimental observations (vida infra).

An apparently spherical small single-crystal Ag nanoparticle is in fact a polyhedron.[30] A truncated octahedron (TO) consisting of eight {111} facets and six {100} facets is a typical morphology for single-crystal Ag nanoparticles (Scheme 1A).[30–32] When the single-crystal silver nanoparticles were subjected to the replacement reaction, Ag atoms were oxidized and dissolved from the nanoparticle surface and $AuCl_4^-$ anions were reduced to Au atoms and deposited on the Ag nanoparticle surface. The dissolution of Ag and the deposition of Au did not occur uniformly on the particle surface. Net growth or etching of specific facets would occur during the reaction, depending on the competition between Au atom deposition and Ag atom dissolution on these facets. Under our experimental conditions, Au deposition occurred initially and preferentially on the high-energy {100} facets. Deposition of Au on the {100} facets impeded the dissolution of Ag from these facets, shifting the Ag dissolution to the {111} facets. The Au atoms deposited on the {100} facets quickly alloyed with the underlying Ag atoms. The alloying of Ag and Au within a nanoparticle due to lattice rearrangement has been investigated in early publications.[10] This rapid alloying of the two metals was facilitated by the combination of reduced particle dimension, interfacial defects, and elevated preparation temperatures.[33–36] The dissolution of Ag atoms from the {111} facets caused these facets to be contracted while the preferential deposition and alloying of Au atoms on the {100} facets led to the protrusion of the latter (Scheme 1B). Figure 2 shows several HRTEM images of the bimetallic nanoparticles at this stage of evolution, as viewed from the ⟨111⟩, ⟨100⟩, and ⟨110⟩ directions, which are consistent with the schematic illustrations below these images. The HRTEM images also show that the protruding alloy tips in the bimetallic nanoparticles were also single crystals.

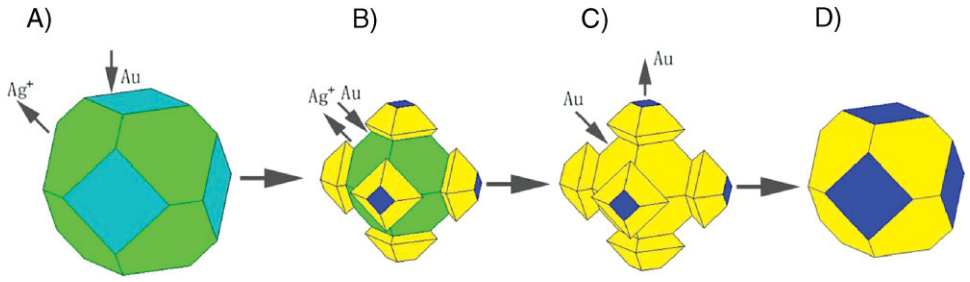

Scheme 1. Schematic illustration showing the shape and composition evolution of Ag@AgAu metal core/alloy shell bimetallic nanoparticles. The green and cyan planes represent the {111} and {100} facets of Ag, respectively; the yellow and blue planes represent the {111} and {100} facets of Ag–Au alloy or pure Au, respectively.

The deposition rate of Au atoms on the {111} facets of silver nanoparticles caught up in the second step of the replacement reaction and became the predominant process. Fast alloying of the deposited Au atoms with the underlying Ag atoms quickly formed an alloy layer on the {111} facets. The deposition of Au atoms on {111} in this instance could be attributed to two reasons. First, the Ag ions released from the replacement reaction could have lowered the growth rate in the [100] direction or increased the rate of growth in the [111] direction. Although the exact reason is not yet known, several groups have previously witnessed such directional sensitivity.[37,38] Second, the reduction in the available area of the {100} facets due to observed tapered growth could also lead to the relative increase in the deposition rate of Au atoms on the {111} facets. Alloying was confined to the surface region since it would be difficult for the deeply seated Ag atoms to diffuse to the surface in the face of an incoming flux of depositing Au atoms. As a result, the alloy layers on the {111} facets were not as thick as those on the {100} facets, leading to the whole particle acquiring the appearance of a nonspherical core/shell nanoparticle (Scheme 1C). Figure 3 shows the HRTEM images of a nanoparticle in this stage of growth as viewed from the ⟨111⟩, ⟨100⟩, and ⟨110⟩ directions, together with the corresponding schematic illustrations.

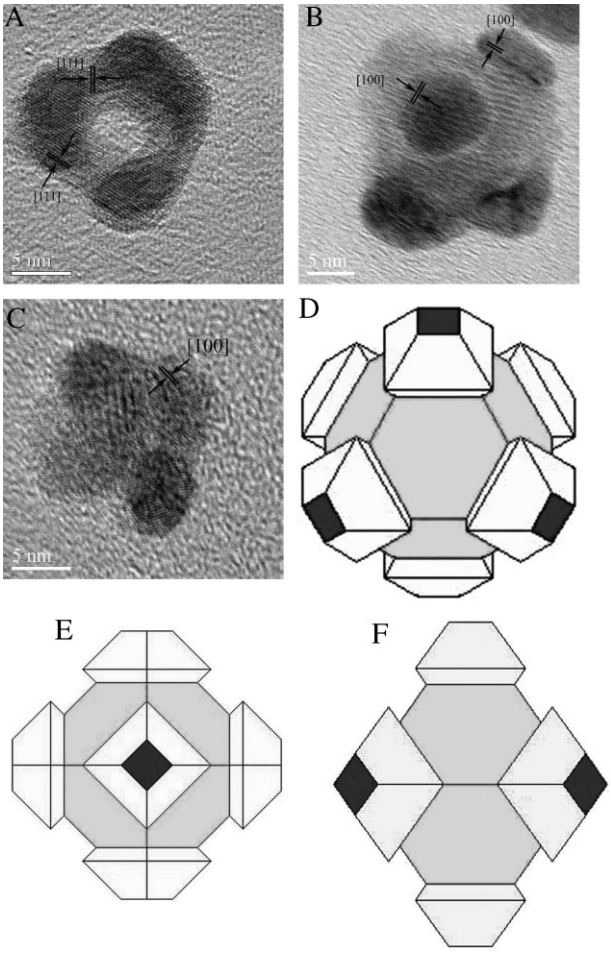

Figure 2. A–C) HRTEM images of bimetallic nanoparticle formed 150 s after the addition of $HAuCl_4$ as viewed from the ⟨111⟩, ⟨100⟩, and ⟨110⟩ directions; D–F) corresponding schematic illustrations of the bimetallic nanoparticles.

With the continuing progress of the replacement reaction, the concentration of $AuCl_4^-$ in the solution and the fraction of leachable Ag in the particle both decreased, leading to the reduction in the rates of Au deposition and Ag dissolution. The rearrangement of surface atoms via Ostwald ripening then became the predominant process. Since TO is a more thermodynamically stable shape for small single-crystal nanoparticles of face-centered cubic (fcc) metals, the atoms in the protruding branches dissolved from the {100} facets and redeposited on the {111} facets to decrease the surface area of the whole particle, resulting in the formation of a core/shell TO nanoparticle (Scheme 1D). The HRTEM images of the core/shell TO nanoparticles (Figure 1G) show that they were perfect single crystals congruent with the schematic illustration in Figure S2. When $HAuCl_4$ was used in stoichiometric excess, as in the case of AgAu-4, the $AuCl_4^-$ in the solution continued to react with the Ag atoms in the alloy shell until the shell was completely devoid of Ag to become a pure Au shell. Different to the case of hollow Au nanoparticles, de-alloying of the alloy shell under our experimental conditions did not lead to the collapse of the shell or the formation of pores in the shell.[28,39]

UV/Vis spectroscopy was also used to follow the evolution of the bimetallic nanoparticles. The UV/Vis spectra underwent significant changes during the conversion of Ag nanoparticle seeds to the bimetallic core/shell nanoparticles. The changes were caused by the combined effects of changes in particle shape, size, composition, and composition distribution. Although the intermediates formed during the replacement reaction were not easily quantifiable, a qualitative

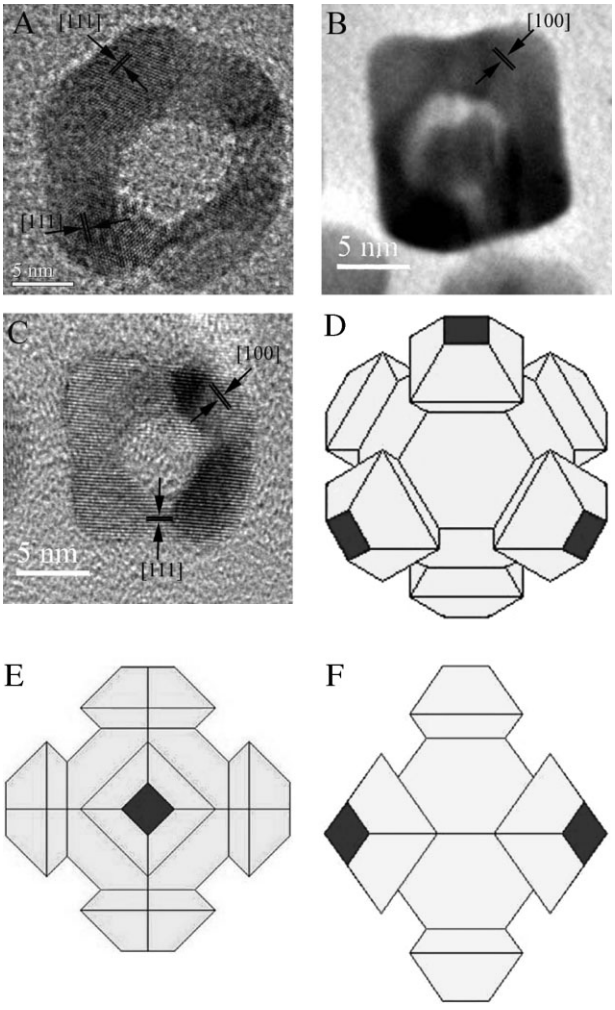

Figure 3. A–C) HRTEM images of the bimetallic nanoparticles formed 360 s after the addition of $HAuCl_4$ as viewed from the ⟨111⟩, ⟨100⟩, and ⟨110⟩ directions; D–F) corresponding schematic illustrations of the bimetallic nanoparticles.

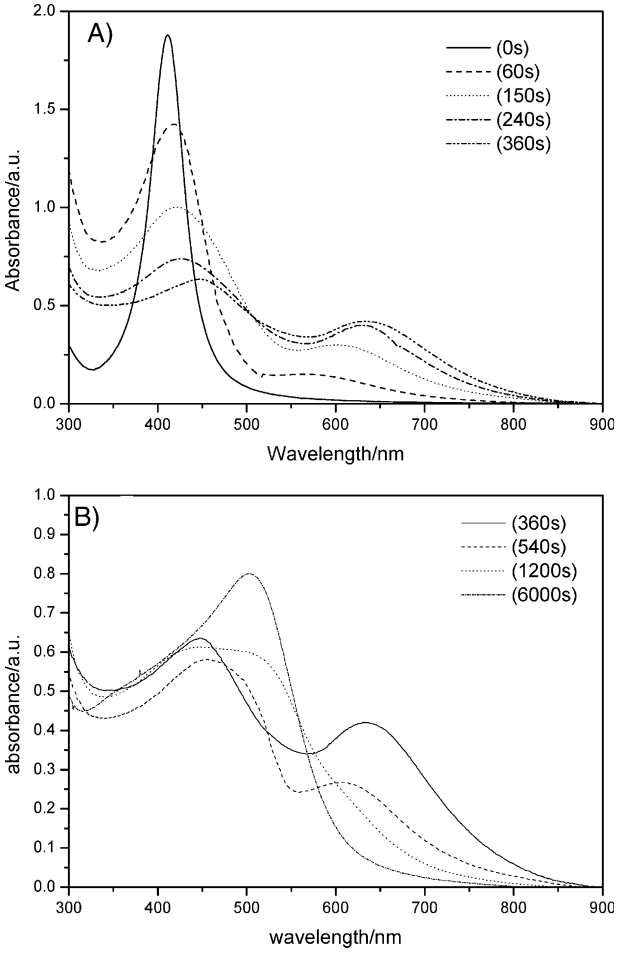

Figure 4. Evolution of the absorption spectra of bimetallic nanoparticles.

understanding of the morphology and composition evolution is still possible by following the spectral changes closely. The starting octadecylamine-protected Ag nanoparticles exhibited the SPR characteristic of the Ag nanoparticles at 409 nm (spectrum 0s in Figure 4A, peak 1). A minute after the addition of $HAuCl_4$, the absorption peak red shifted slightly and the intensity decreased. At the same time a peak appeared at 565 nm (spectrum 60s in Figure 4A, peak 2) and began to red shift with reaction time (spectrum 150s and 240s in Figure 4A). The position of the latter peak was a significant red-shift from the SPR of nonalloyed Ag@Au core/shell nanoparticles (≈530 nm[16]), indicating that Au atom deposition and Ag atom dissolution were not uniform across the particle surface. This is because uniform Au atom deposition and Ag atom dissolution across the surface would lead to core/shell nanoparticles with either a Au shell or a Ag–Au alloy shell; both absorb only at wavelengths shorter than 530 nm. The observation is consistent with the preferential deposition of Au on {100} facets and preferential dissolution of Ag from the {111} facets detected by HRTEM. The appearance of two peaks and their locations are in agreement with the theoretical calculations by plasmon hybridization theory, which states that the surface plasmon of an intermediate bimetallic nanoparticle at this stage can be regarded as the hybrid of a Ag nanosphere (peak 1) and a hexapod-like branched particle (peak 2).[40,41] The position of peak 2 stayed relatively fixed 4 to 6 min after the $HAuCl_4$ addition, while peak 1 continued to red shift (spectrum 360s in Figure 4A). This indicated that Au atoms had started to deposit on the {111} facets and alloyed with the underlying Ag atoms there. The time for this to occur also agreed well with the second step of the replacement reaction. Peak 2 began to blue shift 9 minutes after the addition of $HAuCl_4$ (spectrum 540s, Figure 4B). This could be understood as the shortening of the branches as a result of atomic rearrangement by Ostwald ripening. Meanwhile, the red shifting of peak 1 went unabated because of the increase in the Au fraction on {111} facets. The red shifting of peak 1 and the blue shifting of peak 2 finally collapsed into a common peak (spectrum 1200s & 6000s in Figure 4B), signaling the complete formation of Ag@AgAu bimetallic nanoparticles. The changes in the absorption spectra are consistent with the HRTEM examination, corroborating the proposed mechanism.

In summary, Ag@AgAu metal core/alloy shell bimetallic nanoparticles with tunable shell composition were synthesized by the replacement reaction between Ag nanoparticles and $HAuCl_4$, using small TO Ag nanoparticles as the sacrificial

templates, elevated temperature (95 °C) of preparation, and an aprotic solvent (toluene). The presence of the Ag core and Ag–Au alloy shell was confirmed by selected-area EDX, TEM, HRTEM, and UV/Vis spectroscopy. The composition of the shell was dependent on the Ag to $HAuCl_4$ ratio in the reaction mixture. Time-course studies by HRTEM and UV/Vis spectroscopy revealed the following sequence of events in the evolution of core/shell structures from Ag nanoparticle seeds: 1) oxidative dissolution of Ag atoms from the {111} facets of Ag nanoparticles and initial preferential deposition of Au atoms from $AuCl_4^-$ reduction on the Ag {100} facets, followed by alloying with the Ag atoms below; 2) subsequent Au atom deposition on the Ag {111} facets followed by Ag–Au alloying there; 3) rearrangement of the surface atoms to form the final core/shell nanoparticles.

Experimental Section

A two-step procedure was used to produce Ag nanoparticle templates. The as-synthesized Ag nanoparticles and $HAuCl_4$ were separately transferred to toluene according to previously developed procedures (details in Supporting Information).[42,43] As-prepared Ag organosol (20 mL) was heated to 95 °C and a calculated amount of hydrophobic $HAuCl_4$ (1 mM) was added dropwise to the organosol to prepare Ag@AgAu metal core/alloy shell nanoparticles with different shell compositions. The mixture, which had different colors depending on the shell composition, was cooled down to room temperature, centrifuged to recover the solid product, which was then redispersed in toluene. The bimetallic nanoparticles obtained from the replacement reaction between 20 mL Ag organosol and 2.80, 4.70, 5.80, and 7.00 mL $HAuCl_4$ were labeled as AgAu-1, AgAu-2, AgAu-3, and AgAu-4, respectively. The bimetallic nanoparticles were characterized by TEM, HRTEM, selected-area EDX, and UV/Vis spectrophotometery (Supporting Information).

Keywords:
bimetallic nanoparticles · composition distribution · gold · silver

[1] M. P. Pileni, *Nat. Mater.* **2003**, *2*, 145–150.
[2] I. Lisiecki, D. Parker, C. Salzemann, M. P. Pileni, *Chem. Mat.* **2007**, *19*, 4030–4036.
[3] R. W. J. Scott, C. Sivadinarayana, O. M. Wilson, Z. Yan, D. W. Goodman, R. M. Crooks, *J. Am. Chem. Soc.* **2005**, *127*, 1380–1381.
[4] S. H. Sun, C. B. Murray, D. Weller, L. Folks, A. Moser, *Science* **2000**, *287*, 1989–1992.
[5] M. Grzelczak, J. Perez-Juste, F. J. G. de Abajo, L. M. Liz-Marzan, *J. Phys. Chem. C* **2007**, *111*, 6183–6188.
[6] Y. W. Cao, R. Jin, C. A. Mirkin, *J. Am. Chem. Soc.* **2001**, *123*, 7961–7962.
[7] S. Link, Z. L. Wang, M. A. El-Sayed, *J. Phys. Chem. B* **1999**, *103*, 3529–3533.
[8] M. P. Mallin, C. J. Murphy, *Nano Lett.* **2002**, *2*, 1235–1237.
[9] O. M. Wilson, R. W. J. Scott, J. C. Garcia-Martinez, R. M. Crooks, *J. Am. Chem. Soc.* **2005**, *127*, 1015–1024.
[10] B. Rodriguez-Gonzalez, A. Sanchez-Iglesias, M. Giersig, L. M. Liz-Marzan, *Faraday Discuss.* **2004**, *125*, 133–144.
[11] A. B. Smetana, K. J. Klabunde, C. M. Sorensen, A. A. Ponce, B. Mwale, *J. Phys. Chem. B* **2006**, *110*, 2155–2158.
[12] I. Lee, S. W. Han, K. Kim, *Chem. Commun.* **2001**, 1782–1783.
[13] R. G. Sanedrin, D. G. Georganopoulou, S. Park, C. A. Mirkin, *Adv. Mater.* **2005**, *17*, 1027–1031.
[14] M. Tsuji, N. Miyamae, K. Matsumoto, S. Hikino, T. Tsuji, *Chem. Lett.* **2005**, *34*, 1518–1519.
[15] I. Srnova-Sloufova, F. Lednicky, A. Gemperle, J. Gemperlova, *Langmuir* **2000**, *16*, 9928–9935.
[16] P. Mulvaney, *Langmuir* **1996**, *12*, 788–800.
[17] B. Rodriguez-Gonzalez, A. Burrows, M. Watanabe, C. J. Kiely, L. M. L. Marzan, *J. Mater. Chem.* **2005**, *15*, 1755–1759.
[18] C. H. Chen, L. Subramanyam, J. M. Chen, S. C. Shih, G. R. Wang, D. G. Liu, M. T. Tand, J. F. Lee, B. J. Hwang, *J. Am. Chem. Soc.* **2007**, *1*, 114–125.
[19] Y. G. Sun, Y. N. Xia, *Science* **2002**, *298*, 2176–2179.
[20] Y. G. Sun, B. T. Mayers, Y. N. Xia, *Nano Lett.* **2002**, *2*, 481–485.
[21] P. R. Selvakannan, M. Sastry, *Chem. Commun.* **2005**, 1684–1686.
[22] H. P. Liang, L. J. Wan, C. L. Bai, L. Jiang, *J. Phys. Chem. B* **2005**, *109*, 7795–7800.
[23] Y. D. Yin, C. Erdonmez, S. Aloni, A. P. Alivisatos, *J. Am. Chem. Soc.* **2006**, *128*, 12671–12673.
[24] S. E. Hunyadi, C. J. Murphy, *J. Mater. Chem.* **2006**, *16*, 3929–3935.
[25] X. M. Lu, H. Y. Tuan, J. Y. Chen, Z. Y. Li, B. A. Korgel, Y. N. Xia, *J. Am. Chem. Soc.* **2007**, *129*, 1733–1742.
[26] J. Y. Chen, J. M. McLellan, A. Siekkinen, Y. J. Xiong, Z. Y. Li, Y. N. Xia, *J. Am. Chem. Soc.* **2006**, *128*, 14776–14777.
[27] Q. B. Zhang, J. Y. Lee, J. Yang, C. Boothroyd, J. X. Zhang, *Nanotechnology* **2007**, *18*, 245605.
[28] Y. G. Sun, Y. N. Xia, *J. Am. Chem. Soc.* **2004**, *126*, 3892–3901.
[29] E. Hao, S. Y. Li, R. C. Bailey, S. L. Zou, G. C. Schatz, J. T. Hupp, *J. Phys. Chem. B* **2004**, *108*, 1224–1229.
[30] Z. L. Wang, *J. Phys. Chem. B* **2000**, *104*, 1153–1175.
[31] B. A. Korgel, S. Fullam, S. Connolly, D. Fitzmaurice, *J. Phys. Chem. B* **1998**, *102*, 8379–8388.
[32] S. A. Harfenist, Z. L. Wang, R. L. Whetten, I. Vezmar, M. M. Alvarez, *Adv. Mater.* **1997**, *9*, 817–822.
[33] H. Yasuda, H. Mori, M. Komatsu, K. Takeda, *J. Appl. Phys.* **1993**, *73*, 1100–1103.
[34] T. Shibata, B. A. Bunker, Z. Y. Zhang, D. Meisel, C. F. Vardeman, J. D. Gezelter, *J. Am. Chem. Soc.* **2002**, *124*, 11989–11996.
[35] K. Dick, T. Dhanasekaran, Z. Y. Zhang, D. Meisel, *J. Am. Chem. Soc.* **2002**, *124*, 2312–2317.
[36] D. Das, P. P. Chatterjee, I. Manna, S. K. Pabi, *Scr. Mater.* **1999**, *41*, 861–866.
[37] F. Kim, S. Connor, H. Song, T. Kuykendall, P. D. Yang, *Angew. Chem. Int. Edit.* **2004**, *43*, 3673–3677.
[38] M. Z. Liu, P. Guyot-Sionnest, *J. Phys. Chem. B* **2005**, *109*, 22192–22200.
[39] Y. G. Sun, Y. A. Xia, *Nano Lett.* **2003**, *3*, 1569–1572.
[40] E. Prodan, C. Radloff, N. J. Halas, P. Nordlander, *Science* **2003**, *302*, 419–422.
[41] E. Hao, R. C. Bailey, G. C. Schatz, J. T. Hupp, S. Y. Li, *Nano Lett.* **2004**, *4*, 327–330.
[42] J. Yang, J. Y. Lee, T. C. Deivaraj, H. P. Too, *J. Colloid Interface Sci.* **2004**, *277*, 95–99.
[43] J. Yang, J. Y. Lee, T. C. Deivaraj, H. P. Too, *Colloid Surf. A-Physicochem. Eng. Asp.* **2004**, *240*, 131–134.

Received: December 3, 2007
Revised: February 4, 2008

